Identification of functional lung unit in the dog by graded vascular embolization

IVEN YOUNG, ROBERT W. MAZZONE, AND PETER D. WAGNER
Department of Medicine, University of California, San Diego, La Jolla, California 92093

YOUNG, IVEN, ROBERT W. MAZZONE, AND PETER D. WAGNER. *Identification of functional lung unit in the dog by graded vascular embolization.* J. Appl. Physiol.: Respirat. Environ. Exercise Physiol. 49(1): 132–141, 1980.—To study the dimensions of the functional gas exchange unit, spherical polystyrene beads (diam 50–500 μm) were injected intravenously into 12 normal anesthetized paralyzed dogs (15–24 kg wt). We argued that beads small enough to lodge within gas exchange units would not give rise to a population of high ventilation-perfusion ratio ($\dot{V}_A/\dot{Q}$) areas, whereas embolization of larger vessels supplying these units would. Each dog received only one bead size in cumulative 0.25-g doses up to a maximum of 2.25 g. Multiple inert gas elimination data were obtained after each dose to monitor the development of high $\dot{V}_A/\dot{Q}$ regions. Injection of 50- and 100-μm beads never gave rise to high $\dot{V}_A/\dot{Q}$ regions, whereas 150-, 250-, and 500-μm beads consistently induced a high $\dot{V}_A/\dot{Q}$ mode comprising up to 45% of the ventilation. Histological examination of lungs from five additional dogs injected with small (~0.5 g) doses revealed that beads rarely formed clusters and appeared in vessels of their own diameter in over 90% of instances. By the above criterion, the functional gas exchange unit in these lungs is that volume of tissue subtended by 150-μm-diam arteries (vessels associated with respiratory bronchioles).

gas exchange; inert gases; bead embolization

THE GAS EXCHANGE ABNORMALITIES produced by pulmonary vascular emboli have been studied by a number of investigators using the conventional measurements of arterial blood-gas tensions, alveolar-arterial oxygen pressure ($P_{A_{O_2}}$ -Pa_{O_2}) gradients, and dead space-to-tidal volume ratios V_D/V_T (9–11). Emboli ranging in diameter from 2 to 6 mm [autologous clot emboli (9, 10) to 100-μm glass beads (11)] have been found to cause hypoxemia, hypercapnia, and increases in V_D/V_T and $P_{A_{O_2}}$-Pa_{O_2} gradients. The development of the multiple inert gas infusion technique (5, 19, 17) has enabled a more detailed characterization of the ventilation-perfusion inequalities caused by pulmonary vascular emboli, and it has been found that both autologous clot and glass bead emboli produce a mode of high ventilation-perfusion ratios (3, 15).

A question that arises from such studies is the relationship between the size of the embolus and associated changes in gas exchange. At one extreme, very small emboli (e.g., 15 μm) would not be expected to cause development of high $\dot{V}_A/\dot{Q}$ regions because rich capillary interconnections would allow continued perfusion of the tissue distal to the sites of obstruction. At the other extreme, embolization of a major pulmonary artery clearly results in hypoperfusion (or nonperfusion) of an entire lung, and this does produce areas of high $\dot{V}_A/\dot{Q}$ or increased physiological dead space. These considerations lead to the hypothesis that under a given set of experimental conditions there exists a vessel of critical diameter; embolization of smaller vessels will not produce high $\dot{V}_A/\dot{Q}$ areas, but embolization of larger vessels will. Identification of the size of this vessel then defines (under the particular experimental conditions) the functional unit of lung for gas exchange. Based on theoretical calculations of gas mixing, such a unit is probably subtended by the respiratory bronchiole or first-order alveolar duct (1, 2) in the human lung. The vessels form a similar branching system to the airways in that they run alongside and branch with them (6). However, the size of the vessels supplying these units and the contribution of collateral perfusion to the dimensions of the functional lung unit are unknown.

The purpose of the work described in this paper is *1)* to determine the minimum microembolus size necessary to produce high $\dot{V}_A/\dot{Q}$ areas in the lung using the multiple inert gas infusion technique in normal anesthetized paralyzed dogs and *2)* to identify the size of the corresponding obstructed blood vessels and their associated airways by histological examination of the lungs postmortem.

METHODS

Preparation of Animals

Seventeen mongrel dogs were studied in the supine position. They were all anesthetized with pentobarbital (30 mg/kg) and relaxed with gallamine (60–100 mg). Further doses of pentobarbital and gallamine were given during the experiment to maintain an absent corneal reflex and complete relaxation. Heparin, 5–10 × 10^3 U, was injected before the first dose of beads, then 2–5 × 10^3 U were injected every 30 min during the experiment. Each animal was ventilated using a volume cycled respirator set to maintain an end-tidal carbon dioxide tension (P_{CO_2}) of approximately 30 Torr before any experimental insult (frequency ~14 Hz, V_T ~300 ml). This initial pattern of ventilation was maintained throughout each experiment and a constant end-expiratory pressure of 5 cmH_2O was applied to the expired line throughout the study.

A 7F-gauge Swan-Ganz flotation catheter was passed into the pulmonary artery via a jugular vein, and wide-bore catheters placed in a femoral artery and a femoral

0161-7567/80/0000-0000$01.25

vein. The pulmonary artery catheter was used to sample mixed venous blood and measure pulmonary artery pressure; the femoral artery catheter was used to sample systemic arterial blood and monitor systemic pressure. The femoral venous catheter (passed well into the inferior vena cava) was used to inject each bolus of beads. A narrow catheter was inserted into a peripheral leg vein to infuse the solution of dissolved inert gases (see below). Expired P_{O_2} and P_{CO_2} were monitored with a respiratory mass spectrometer (Perkin-Elmer MGA 1100), and all signals were displayed on a Brush recorder (Gould Instruments).

Preparation of Beads

Polystyrene spherical ion exchange resin beads (BioRad Laboratories) were used as emboli because they section easily in tissue embedded in paraffin and stain well with hematoxylin. Prior to injection into each animal, they were sorted into five size ranges (approx diam 50, 100, 250, and 500 μm) using US standard sieves (Scientific Products). The beads were suspended in normal saline and then washed through the sieves, the beads sticking to the mesh of each size sieve being retained. They were then oven-dried at 37°C, which caused some shrinkage and allowed them to be brushed out. On resuspension in 0.9% saline, the beads regained their original wet sizes within 15–30 s.

Prior to each experiment, a small sample of the beads to be used was suspended in saline and the diameters of 50 randomly selected beads measured using a microscope with eyepiece graticule. The mean ±SD diameters of the beads used in each experiment and the overall mean ±SD of each size used are listed in Table 1.

Beads were injected as 0.25 gram doses (weighed dry), so samples of 50 dry beads in each range were also sized to obtain an approximate number of beads for each 0.25-g dose. The density of the polysytrene material (1.05 g/cm^3) was obtained from the manufacturer. The number of beads in one 0.25-g dose of each size range was calculated using the formula: number of beads = $(2 \times 0.25)/(4.2 \times \pi \times [D/2]^3)$, where D is the measured mean diameter in centimeters. There were approximately 7.463×10^6 50-μm beads, 7.637×10^5 100-μm beads, 3.528×10^5 150-μm beads, 5.983×10^4 250-μm beads, and 1.133×10^4 500-μm beads in each 0.25-g dose.

Experimental Protocol

A solution of the six inert gases, sulfur hexafluoride (SF_6), ethane, cyclopropane, halothane, ether, and acetone in 0.9% saline was infused at 2.5 ml/min. The theory of the multiple inert gas technique has been described (5, 18), as have the practical details (15–17). Each animal was judged to be in a steady state from the end-tidal P_{O_2} and P_{CO_2} and measurements. This was confirmed subsequently by constancy of tidal volume and frequency, arterial and mixed venous P_{O_2} and P_{CO_2}, and cardiac output. Mixed venous and arterial blood samples and mixed expired gas samples were then drawn, and retention and excretion values of the inert gases were calculated (17, 18). Duplicate samples were taken at this time to provide two base-line $\dot{V}_A/\dot{Q}$ distributions before the beads were injected.

TABLE 1. *Measured wet bead diameters*

	50 μm	100 μm	150 μm	250 μm	500 μm
Individual expt means	56.4 ±4.5	117.8 ±11.6	145.4 ±22.8	268.5 ±18.4	482.8 ±18.6
	64.0 ±5.8	114.2 ±16.2	149.6 ±8.3	263.9 ±27.5	485.4 ±15.8
	55.2 ±5.0	117.8 ±11.0	161.3 ±9.6	273.3 ±21.3	477.8 ±12.0
	60.1 ±5.4			274.6 ±20.9	
Overall means	58.9 ±5.2	116.6 ±13.1	152.1 ±14.4	270.1 ±22.3	482.0 ±15.7

Values are means ± SD, given in μm.

In 12 of the 17 dogs, 0.25-g boluses of beads in one size range only were injected (*group A*). Nine such doses were used in most cases for a total dose of 2.25 g. Fifteen minutes after each injection, a steady state was regained as judged by the end-tidal gas tension and blood pressure traces, and blood and gas samples were withdrawn for inert gas analysis and measurement of P_{O_2}, P_{CO_2}, and pH.

Dog 1 was the first studied. It was injected with only 0.1-g boluses of 50-μm beads because of the large number of these beads per unit weight. However, there was only a modest rise (11 Torr) in mean pulmonary artery pressure, so all subsequent dogs were given 0.25-g boluses. Three animals died before the total dose had been administered (*dogs 5, 15,* and *16*).

A different protocol was used for the remaining five dogs (*group B*), which were injected with a single bolus (0.75 or 0.5 g) of beads in one size range. This produced only modest increases in mean pulmonary artery pressure (Table 2). They were then killed after inert gas samples were taken, and their lungs were fixed, sectioned, and examined for sites of bead deposition. This separate protocol was used because the dogs subjected to the full dose had high pulmonary artery pressures after the last dose, so that later beads lodged more peripherally than beads given earlier. The location of the beads in the *group B* dogs was then correlated with the development of areas of high $\dot{V}_A/\dot{Q}$ as detected by the inert gas method.

Preparation of Lung Tissue (Group B Dogs)

Following the last blood collection for inert gas analysis, the dogs were killed with a venous injection of saturated KCl. The lungs were removed and inflated to 20 cmH_2O pressure via the airways with buffered formaldehyde solution for approximately 1 wk. Sections 0.5–1.0 cm thick were then cut from the ventral aspects of the upper lobes and the dorsal aspects of the lower lobes, four sections from each animal. Each section was fixed for a further 3–7 days in formaldehyde solution, embedded in paraffin, sectioned, and stained with hematoxylin and eosin. Five 5-μm-thick sections were taken from each block, approximately equally spaced through the thickness of the block.

The sectioned beads (stained magenta) were easily

TABLE 2. *Maximum changes in physiological variables with embolization*

Dog No.	Wt of Dogs, kg	Bead Diam, μm	Total Mass of Beads Injected, g	Max Increase in Shunt, %$\dot{Q}_T$	Max Increase* in $\dot{V}$ to a Separate High Mode, %$\dot{V}$tot	Max Change* in $\dot{V}_D$, %$\dot{V}$tot	Max Increase* in Mean PAP, Torr	Max Change in $\dot{Q}_T$, l/min
1	20.0	50	0.90	0.0	0.0	−10	11	−0.5
2	18.8	50	2.25	15.0	0.0	−20	35	−1.9
3	21.0	50	2.25	21.0	0.0	−9	41	−2.9
4†	21.5	50	0.75	1.0	−2.0	−5	12	0.1
5	15.0	100	1.75	9.0	0.0	7	35	−1.4
6	20.8	100	2.25	0.0	0.0	−15	16	−1.8
7†	17.2	100	0.75	1.5	−4.0	−7	15	0.0
8	19.9	150	2.25	9.0	25.0	10	33	−0.9
9	22.2	150	2.25	7.0	22.0	0	37	−0.3
10†	20.0	150	0.75	7.0	5.0	5	26	−0.7
11	19.6	250	2.25	21.0	23.0	−5	50	−0.9
12	24.0	250	2.25	7.0	16.0	9	33	−2.3
13	22.2	250	2.25	12.0	17.5	−10	36	−0.3
14†	25.5	250	0.75	5.0	15.0	−6	11	−0.9
15	19.0	500	1.75	38.0	45.0	−10	41	1.7
16	20.0	500	2.00	9.0	39.0	8	39	0.9
17†	18.8	500	0.50	0.5	11.0	−6	12	0.2

$\dot{Q}_T$, cardiac output; $\dot{V}$, ventilation; %$\dot{V}$tot, percent of total ventilation; $\dot{V}_D$, dead-space ventilation; PAP, pulmonary artery pressure. * Maximum change from base-line values. Change in any direction had to be sustained for more than one measurement to be noted. † Dogs used for histology.

located in the vessels, and each blocked vessel was classified according to the number of beads seen blocking it. As each dog had only one size bead injected, the number of beads seen in the vessel section provided a measure of the size of vessel blocked, even though different planes of section made the beads appear to be different sizes.

RESULTS

Physiological Changes with Progressive Embolization

Base-line measurements. The results for all 17 dogs studied are summarized in Table 2. Dogs are grouped according to bead size injected. The last dogs in each bead size group (*dogs 4, 7, 10, 14,* and *17*) were those that were injected with a single smaller mass of beads for subsequent detailed histological examination (single-dose protocol *group B* dogs). In all dogs, distributions measured before bead injection contained virtually all of the pulmonary blood flow and one-half to two-thirds of the ventilation distributed narrowly around a $\dot{V}_A/\dot{Q}$ ratio of 1. The remaining ventilation was of deadspace (unperfused lung). Shunt never exceeded 5% of the cardiac output, and in a few dogs high $\dot{V}_A/\dot{Q}$ regions (no more than 9% of ventilation) were observed. Appearance of high $\dot{V}_A/\dot{Q}$ regions under control conditions almost certainly reflects relatively low pulmonary artery pressures with the uppermost regions having little or no perfusion. Similar patterns are seen with positive end-expiratory pressure ventilation (4) and appear when pulmonary artery pressure is less than alveolar pressure. These regions of high $\dot{V}_A/\dot{Q}$ tended to disappear as pulmonary artery pressure rose after the first 0.25-g dose of beads.

Measurements following embolization. Mean pulmonary artery pressure increased greatly in all animals receiving large doses of beads. The increase was almost linear with respect to bead dose in most animals. The cardiac output fell during most experiments, although this response was variable. There was a rise in the shunt fraction of the cardiac output (Figs. 1–5). In nine animals there were also low $\dot{V}_A/\dot{Q}$ (<0.05) units contiguous with the shunt compartment, but the exact proportion of each cannot be determined (5). Regions of shunt and low $\dot{V}_A/\dot{Q}$ were grouped together for Figs. 1–5 and labeled shunt in Table 1.

A separate high $\dot{V}_A/\dot{Q}$ mode developed in all dogs (*nos. 8–17*) that were injected with 150-μm or larger beads. The dogs injected with 50- or 100-μm beads (*nos. 1–7*) developed no separate high $\dot{V}_A/\dot{Q}$ mode after bead injection, even up to the maximum total amount of 2.25 g (approx 6.7×10^6 100-μm beads). Figures 1–5 summarize the development of high $\dot{V}_A/\dot{Q}$ regions measured in five representative dogs, each injected with a different bead size. The small fraction of ventilation to a separate high mode in *dog 3* (Fig. 1) disappeared after the third dose of beads, as the pulmonary artery pressure rose. None of the 50-μm bead dogs developed either a high $\dot{V}_A/\dot{Q}$ mode or widening of the main mode with successive doses of beads.

Similar findings are illustrated in Fig. 2 for a representative 100-μm bead dog (*no. 6*). No high $\dot{V}_A/\dot{Q}$ regions developed in this, or the other 100-μm bead dogs.

The injection of 150-μm beads resulted in the appearance of a separate high $\dot{V}_A/\dot{Q}$ mode in both full-protocol dogs injected. The results for *dog 9* are illustrated in Fig. 3. On the average, the high $\dot{V}_A/\dot{Q}$ mode contained 24% of the total ventilation. Animals injected with 250- and 500-μm beads also developed a separate high $\dot{V}_A/\dot{Q}$ mode, illustrated in Fig. 4 (*dog 11,* 250-μm bead emboli) and Fig. 5 (*dog 15,* 500-μm bead emboli). Ventilation of these modes averaged 19% of the total ventilation in the three 250-μm bead full-protocol dogs, and 41% in the two 500-μm bead full-protocol dogs.

Histological Findings

The 20 histological sections cut from the lungs of each of the single-dose protocol (*group B*) dogs (*nos. 4. 7, 10, 14,* and *17*) yielded the results summarized in Table 3. Each bead-containing vessel was classified according to the number of beads seen in the lumen and whether they were arranged in line (1, 2 × 1, 3 × 1, 4 × 1, . . .) or in groups, two or more beads wide (2 × 2, 3 × 2, . . . , 7 × 2). In the entire study, only two vessels were seen in sections from one dog (*no. 10*) having collections of beads as large as two wide by four and six beads long, respectively. The beads were not always cut through maximum diameter but were assumed to be within the size ranges designated in the first column of Table 3.

Table 3 demonstrates that the majority of vessels were blocked by either single beads or collections only one bead wide, and that therefore the physiological effects, at least in the single-dose protocol dogs, can be attributed to the blocking of vessels in the same size range as the particular beads.

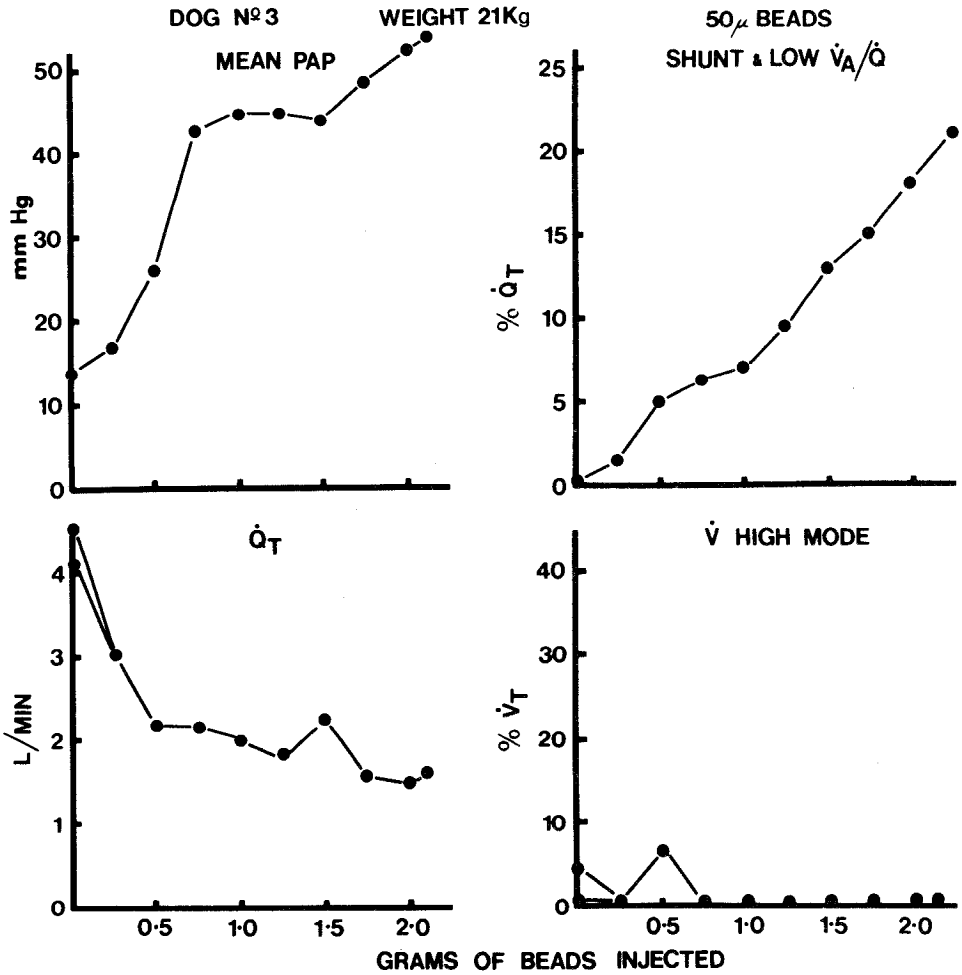

FIG. 1. Changes in mean pulmonary artery pressure (PAP), regions of shunt and low $\dot{V}_A/\dot{Q}$ ratio, regions of high $\dot{V}_A/\dot{Q}$ ratio and cardiac output ($\dot{Q}_T$) are shown after successive boluses of 50-μm beads were injected into *dog 3*. Duplicate values are shown for base-line conditions.

One section from each of the single-dose protocol dogs is shown in Figure 6. Examination of all tissue sections from these dogs revealed that all of the 50-μm and most of the 100-μm beads lay in the parenchyma not associated with airways, whereas beads 150 μm and larger were strikingly associated with bronchioles. On the other hand, the 50- and 100-μm beads were lodged well into the alveolar parenchymal tissue and, in general, were not related to small airways. This striking association (Fig. 6) provides good evidence that it is necessary to occlude vessels that accompany respiratory bronchiles before reduction in local blood flow measurably alters gas exchange.

Each tissue block taken included at least one pleural surface, so measurements could be made of how peripherally beads of a given size lodged. At least two tissue sections for each bead size were examined, and the perpendicular distance from the pleural surface was measured for at least 50 beads in each size range. The 50-μm bead sections revealed that 4% of beads were within 25 μm of the pleural surface, 16% within 500 μm, 40% within 1 mm, and all within 4 mm of the pleural surface. Only 2% of vessels blocked were associated with alveolar ducts; the others were not associated with any conducting airway.

The tissue sections with 100-μm beads showed 4% lying within 25 μm, 18% within 500 μm, 24% within 1 mm, 46% within 2 mm, 70% within 3 mm, 84% within 4 mm, and all within 7 mm of the pleural surface. Thirty-one percent of the blocked vessels were associated with alveolar ducts, 19% with respiratory bronchioles, and 8% with small bronchioles (diam <1 mm). The remaining 42% lodged in the parenchyma, some possibly in supernumerary pulmonary arteries (6). These were vessels unassociated with airways.

The tissue sections with 150-μm beads revealed no beads within 25 μm of the pleural surface, only 8% within 500 μm, 39% within 2 mm, and 67% within 5 mm of the pleural surface. The remaining 33% lodged in regions up to 1 cm from the pleural surface. The majority (53%) of vessels blocked by 150-μm beads were associated with respiratory bronchioles, 19% with alveolar ducts, and 17% with small bronchioles. The remaining 11% of vessels were not associated with any airways in the particular sections. Presumably, these would be supernumerary vessels (6).

The 250-μm bead tissue sections revealed that no beads lodged within 500 μm of the pleural surface. Only 7% of beads were within 1 mm, 44% within 2 mm, and 78% within 5 mm of the pleural surface. The remaining 22% were in large vessels far from the pleural surface. Seventy-eight percent of vessels blocked were associated with small bronchioles, 11% with respiratory bronchioles, and 4% with alveolar ducts, and the remaining 7% of blocked vessels did not appear to be associated with bronchioles in the section. Again, these last vessels may be supernumerary arteries (6).

The 500-μm bead sections could be scanned with the

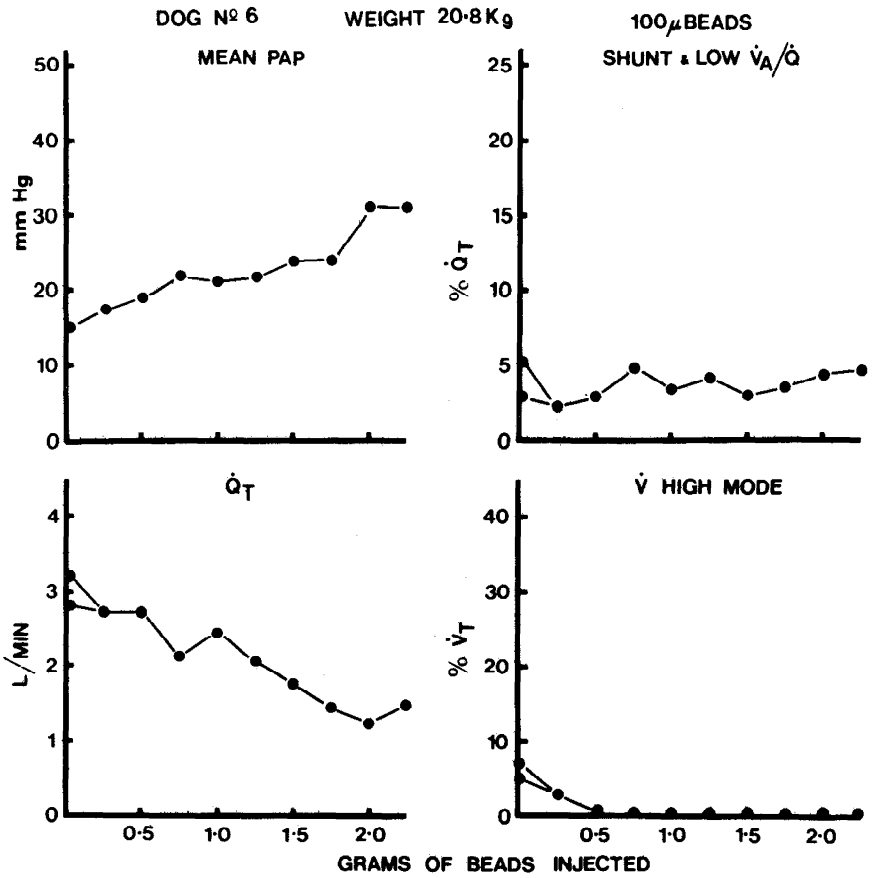

FIG. 2. Same measurements as those displayed in Fig. 1 are shown for *dog 6*, injected with 100-μm beads.

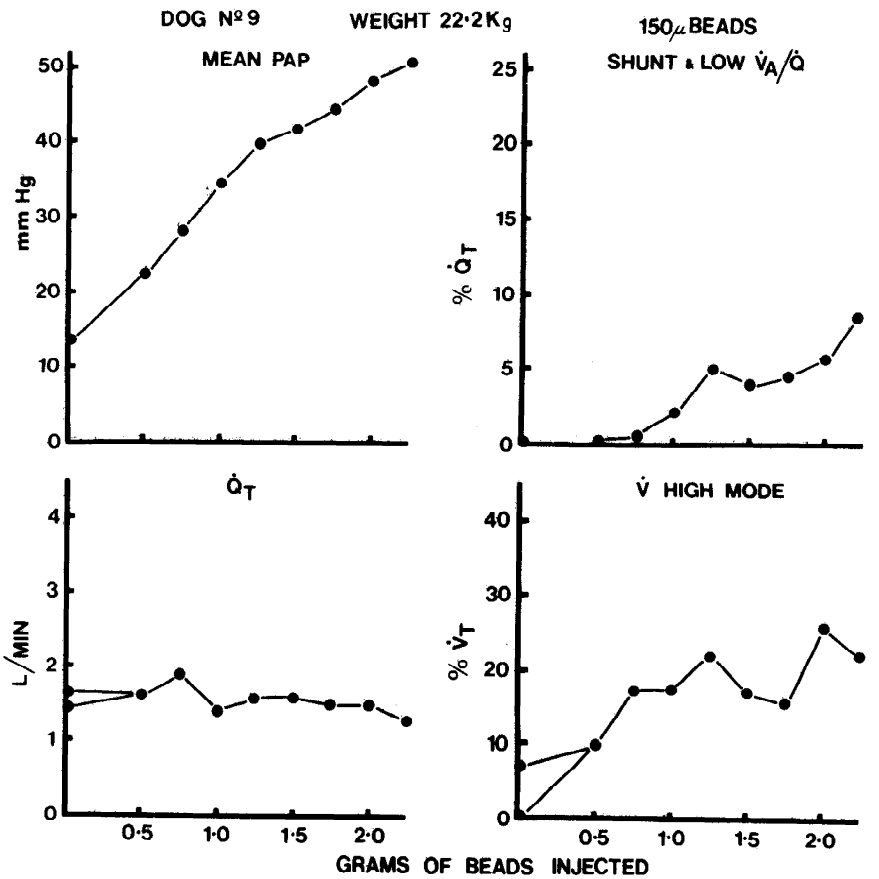

FIG. 3. Same measurements as those displayed in Fig. 1 are shown for *dog 9*, injected with 150-μm beads.

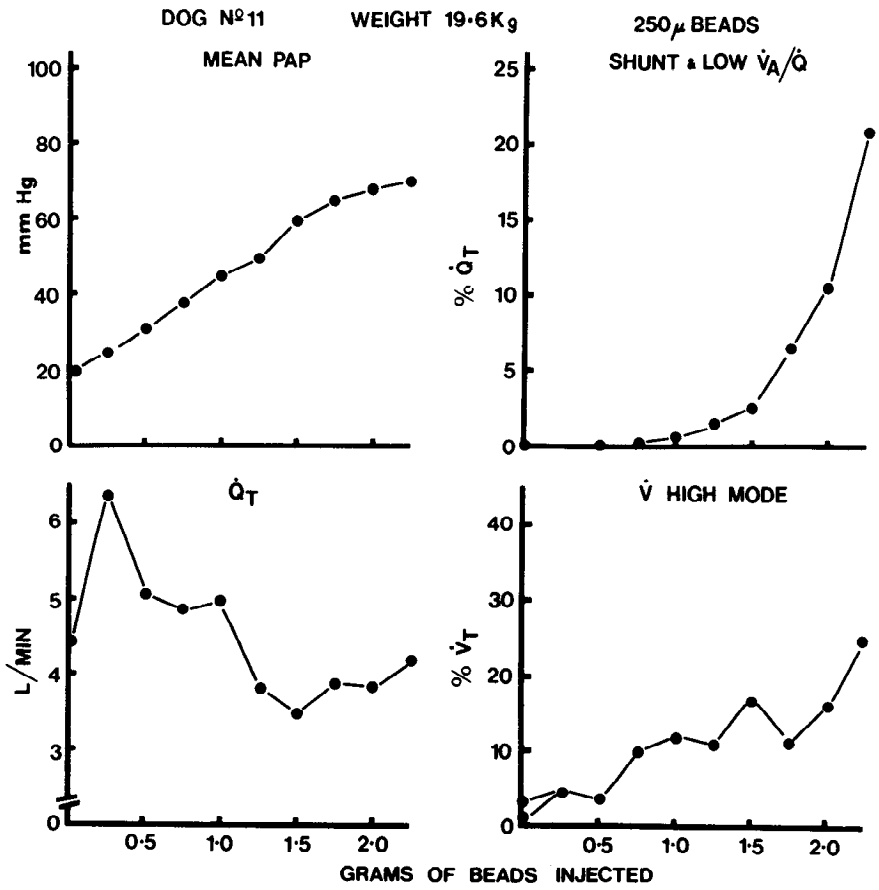

FIG. 4. Same measurements as those displayed in Fig. 1 are shown for *dog 11*, injected with 250-μm beads.

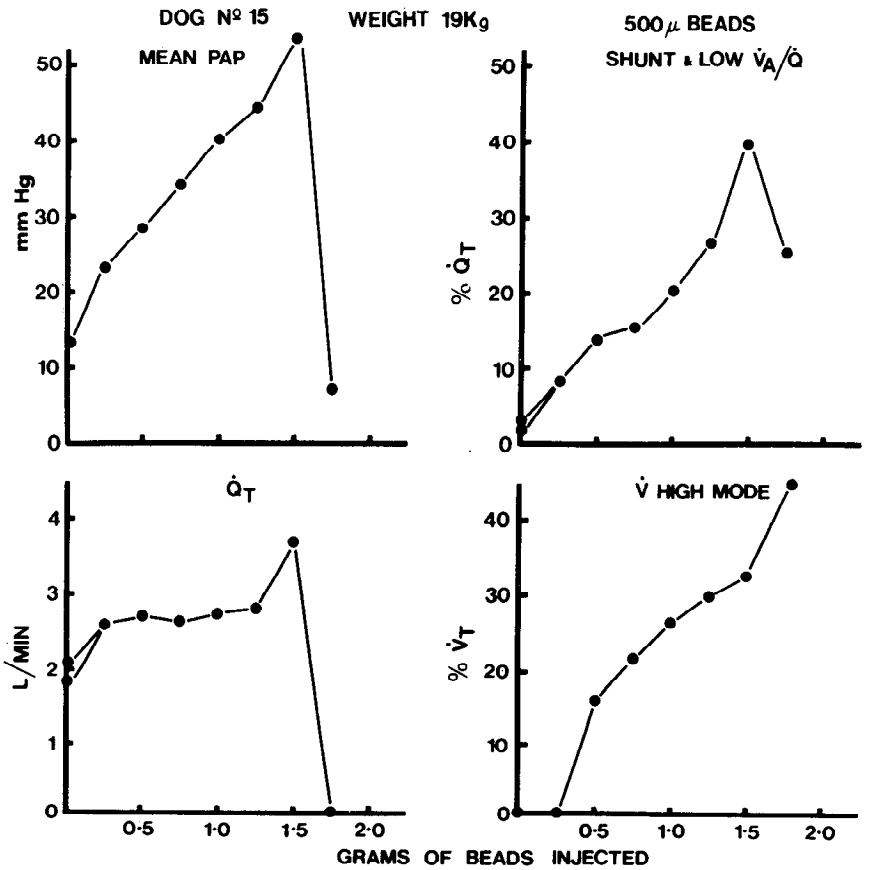

FIG. 5. Same measurements as those displayed in Fig. 1 are shown for *dog 15*, injected with 500-μm beads.

TABLE 3. *Bead aggregation in five single-dose protocol dogs*

Bead Size, μm	Bead Aggregate Size																Total	% of Total	
	Single-bead width								2- or 3-bead width									Single-bead width	2- or 3-bead width
	1	2×1	3×1	4×1	5×1	6×1	7×1	8×1	2×2	3×2	4×2	5×2	6×2	7×2	*n*×2	*n*×3			
50	1,677	228	59	24	8	4	1		17	12	8	5	2		1(10×2) 1(12×2)		2,047	97.8	2.2
100	459	142	41	10	8	2	4	1	9	4	2				1(9×2)		683	97.7	2.3
150	217	66	20	8	3	1	4	2	30	5	9		2	2	2(10×2) 1(8×2)	2(6×3) 1(4×3)	372	86.3	13.7
250	187	57	8	2	2				11	1	1						269	95.2	4.8
500	44	15	7		1			1		1							69	98.6	1.4

For each bead size, it is shown how beads were deposited in blood vessels (singly and in aggregates of various size). Note that very few vessels contained more than one bead across.

naked eye, and all blocked vessels were associated with bronchioles (diam <1 mm).

In summary, all 50-μm and 84% of 100-μm beads (beads that did not cause high $\dot{V}_A/\dot{Q}$ regions) lodged within 4 mm of the pleural surface, and all of 50-μm and 82% of 100-μm beads lay in vessels associated with either alveolar duct or parenchymal tissue. By contrast, 150-μm beads were not as close to the pleural surface, and 53% lay in vessels associated with respiratory bronchioles. Seventeen percent were associated with small nonrespiratory bronchioles. Finally, 250- and 500-μm beads lay still more centrally, and 78 and 100%, respectively, were seen in vessels associated with small bronchioles. Only 11 and 0%, respectively, were associated with respiratory bronchioles. These associations are summarized in Fig. 7.

DISCUSSION

Size of Functional Lung Unit

The basic question examined in this paper is what is the smallest pulmonary artery that must be occluded to measurably produce areas of high $\dot{V}_A/\dot{Q}$ as a result of decreased perfusion. The multiple inert gas elimination technique is able to detect units with impaired blood flow as a collection of units with high $\dot{V}_A/\dot{Q}$, whereas those units not blocked by the emboli retain $\dot{V}_A/\dot{Q}$ values in the normal range (15). The data in Table 3 and Fig. 6 indicated that the vessels occluded by a given size bead had the same diameter as the bead in the great majority of instances in the single-dose protocol dogs.

The clear appearance of high $\dot{V}_A/\dot{Q}$ units following injection of 150-μm beads is, then, good evidence that vessels of about this size supply the functional lung unit under the present experimental conditions.

For the most part, beads of 100-μm diameter or less that did not produce high $\dot{V}_A/\dot{Q}$ regions were found close to the pleural surface and not associated with conducting airways. Beads of 150-μm diameter were generally associated with respiratory bronchioles (Fig. 6), whereas 250-μm and larger diameter beads were associated with small nonrespiratory bronchioles. These associations further define the magnitude of the functional lung unit under the present conditions, as that tissue distal to respiratory bronchioles.

A question that must be considered is whether or not a 150-μm-diameter vessel is compatible with a respiratory bronchiole. In the cat lung, Rhodin (14) has found that vessels associated with respiratory bronchioles may be on the order of 30–160 μm. In the human lung, Hislop and Reid (6) have stated that partially muscular and nonmuscular vessels may be found up to a diameter of 150 μm at the alveolar level. We have examined vessels associated with respiratory bronchioles in rapidly frozen normal dog lung. Unpublished measurements of 60 randomly selected vessels reveal a mean diameter of 140.3 ± 43.0 μm. Thus, it would appear that vessels associated with respiratory bronchioles can vary in size and that our findings in this study are reasonable.

We must also consider whether the beads used in our study could have appeared in smaller vessels due to pulmonary artery hypertension. We would discount this possibility because the histological measurements were performed on the single-dose protocol dogs. In some of these animals there was a sufficient rise in pulmonary artery pressure to suspect bead displacement. Furthermore, if bead displacement as a result of hypertension had occurred, we would have probably seen disruption in the vessel. This was never noted and, in fact, there were often gaps between the beads and the vessel wall.

Alternative Interpretations

We have assumed that 50- and 100-μm beads failed to produce units with high $\dot{V}_A/\dot{Q}$ because they were deposited within the gas exchange units. There are two other possible explanations. First, functional lung units may indeed be supplied by 50- or 100-μm-diameter vessels, but we may not have blocked enough of them by injecting 2.25 g of beads to create measurable regions of high $\dot{V}_A/\dot{Q}$. We feel this possibility can be dismissed. The total number of 50-μm beads in 2.25 g is approximately 67×10^6, and there are approximately 7×10^6 100-μm beads in 2.25 g. The very large increases in pulmonary artery pressure in these dogs (fatal in *dog 5*) indicated that large proportions of the pulmonary bed were occluded without any appearance of high $\dot{V}_A/\dot{Q}$ regions.

A second possibility is that 50- and 100-μm beads did create high $\dot{V}_A/\dot{Q}$ units transiently, but the ventilation was reflexly directed away from these units and redistributed in accord with the redistribution of blood flow (10). Since the $\dot{V}_A/\dot{Q}$ distribution did not widen in these dogs, a very fine control would have to be postulated, and it would also have to be assumed that beads of 150-μm

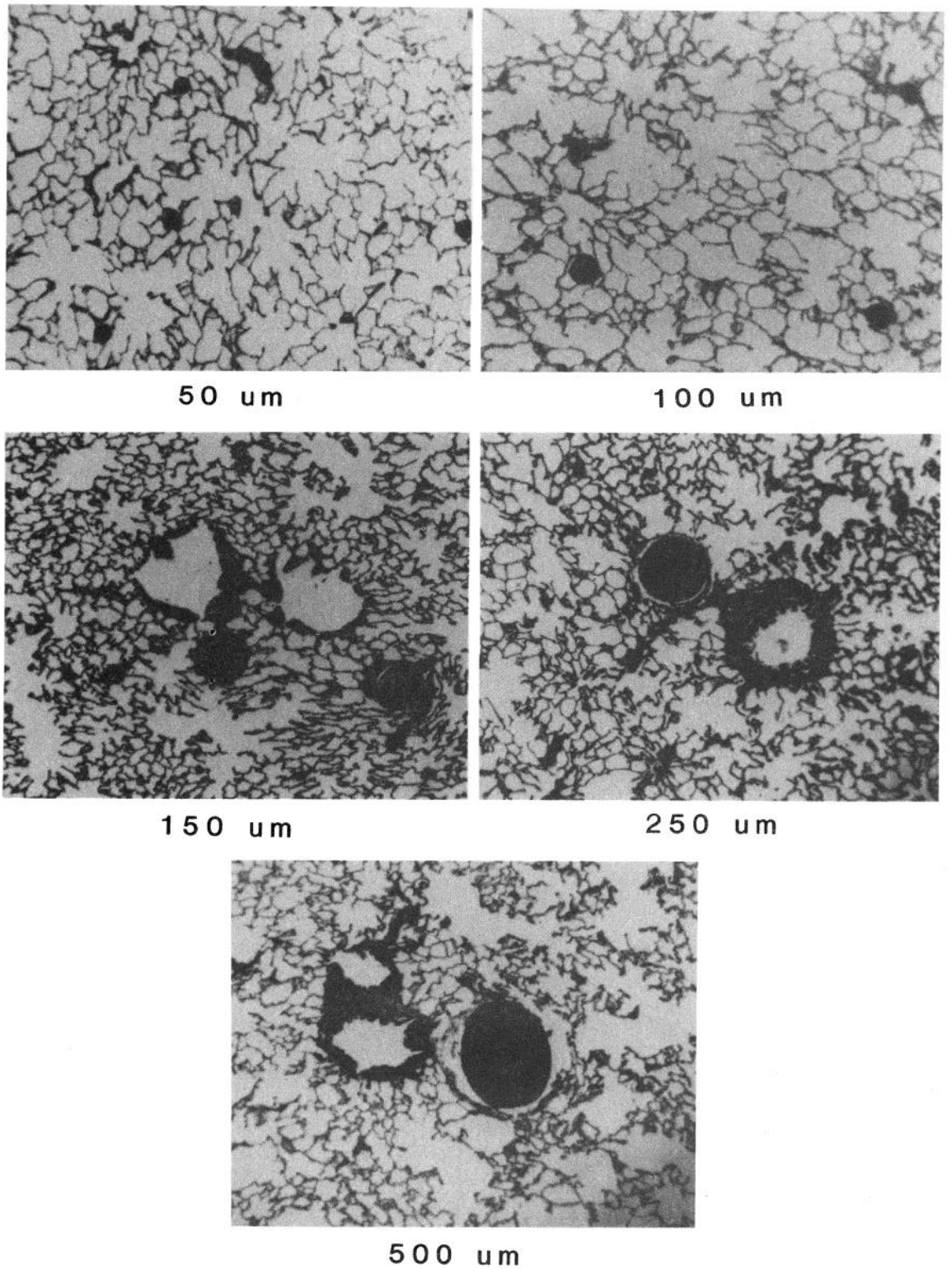

FIG. 6. Photomicrographs of five sections taken from each of the 5 single-dose protocol dogs. Position of 150-μm and larger beads in vessels accompanying bronchioles is discussed in the text.

diameter and greater do not have this effect—two conditions whose coexistence seems unlikely.

It is also possible that the high $\dot{V}_A/\dot{Q}$ mode we found with the 150-μm beads was due to reflex or humoral constriction of even larger vessels. However, two studies suggest that the larger beads (over 250 μm in diameter) do not cause remote reflex effects on the pulmonary vasculature. Niden and Aviado (13) found that glass beads less than 250 μm in diameter caused remote pulmonary vascular constriction, whereas larger beads did not; Kealey and Brody (8) measured a fall in vascular resistance in nonembolized lung when beads less than 100 μm in diameter were injected but not after injection of 130-μm beads. Thus, it is unlikely that the $\dot{V}_A/\dot{Q}$

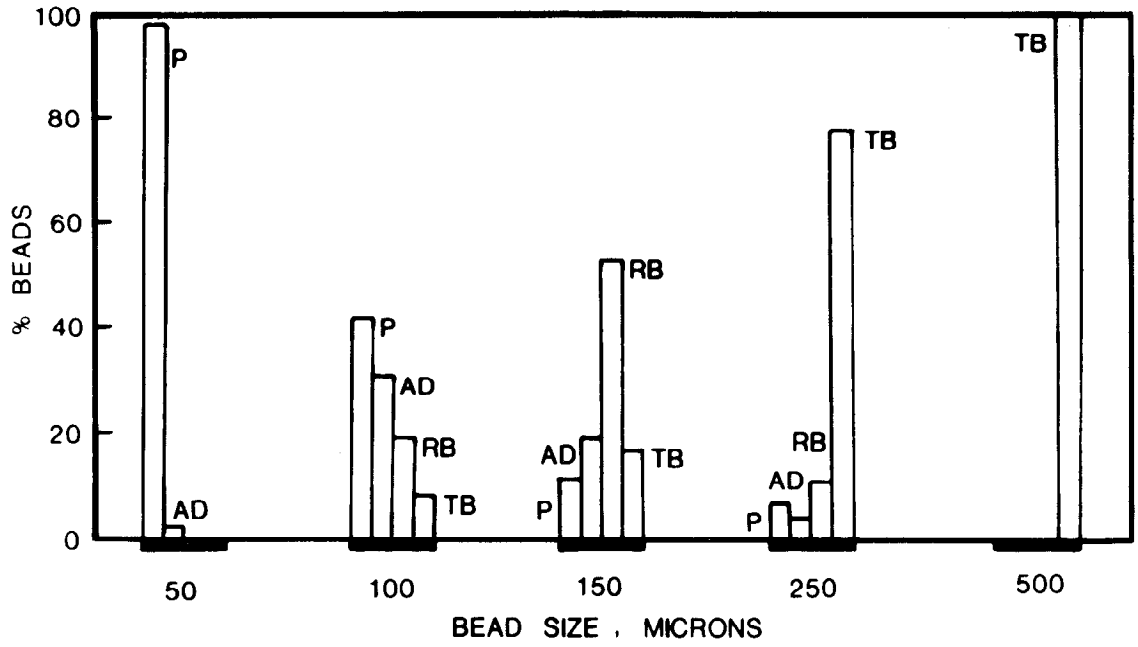

FIG. 7. Airways associated with deposited beads. Beads of a given size were found in vessels associated with parenchymal tissue (P), alveolar duct (AD), respiratory bronchioles (RB), and terminal bronchioles (TB). Each *vertical bar* indicates these associations percentagewise. Small beads (50 μm) appear mostly in the parenchyma. Large beads (500 μm) appear mostly in vessels associated with terminal bronchioles. Most of 150-μm beads are associated with respiratory bronchioles.

changes induced by our large beads were due to remote reflex effects on larger vessels. In addition, the dogs in the present study were well heparinized in an attempt to prevent such effects on the basis of humoral agents.

Increase in Shunt and Physiological Dead Space

The mechanism of the increase in shunt fraction is of interest. There is a significant positive correlation with increase in mean pulmonary artery pressure (Table 2, $R = 0.75$, $P < 0.05$), and the production of pulmonary edema may be the responsible mechanism. Alveoli filled with edema fluid were seen in tissue sections from the full-protocol (*group A*) dogs. There was very little increase in shunt in the single-dose protocol dogs (Table 2), and no pulmonary edema seen in the tissue sections from these dogs. Malik and van der Zee (12) found that embolization with 100-μm glass beads failed to increase the shunt fraction measured during administration of 100% O_2 in heparinized dogs. In dogs that did not receive heparin, however, the shunt fraction increased on average by 8%, and there was also an increase in extravascular lung water. Malik and van der Zee concluded that humoral factors released from platelets caused these differences. The large increases in shunt and pulmonary edema in our well-heparinized dogs therefore suggest other than humoral factors. One possible reason for the discrepancy between the two studies is the larger increases in mean pulmonary artery pressure in our dogs. Malik and van der Zee induced rises of only 15 to 20 Torr in pulmonary artery pressure, whereas our dogs developed increased of from 11 to 50 Torr. Those dogs that developed less than a 20-Torr increase in pulmonary artery pressure showed less than a 2% increase in shunt (*dog 1, 4, 6, 7, 17,* and *21*), except *dog 14*, which developed a 5% increase in shunt with an increase in pulmonary artery pressure of 11 Torr. Those dogs with large shunts (>12%, Table 2) increased their pulmonary artery pressure by at least 35 Torr.

It is also interesting to note that Malik and van der Zee measured increases in V_D/V_T of from 15 to 30% in both heparinized and nonheparinized dogs. This suggests the appearance of high $\dot{V}_A/\dot{Q}$ regions in their dogs of similar weight (approx 20 kg) with 100-μm bead emboli. It is possible that the 100-μm glass beads used in their study aggregated to block larger than 100-μm vessels, and the injection of an average of 14 g of these beads per animal may have contributed to their aggregation, even though they were infused over a 5-min period. A second factor that may have contributed to the elevated V_D/V_T ratios is the rise in arterial P_{CO_2} caused by the development of low $\dot{V}_A/\dot{Q}$ regions or shunt (rather than the changes induced by high $\dot{V}_A/\dot{Q}$ areas).

We are grateful to Carlita M. Durand and Frank Carlton-Lopez for their technical assistance and to Tania Davisson for preparation of the manuscript.

This study was supported by National Heart, Lung, and Blood Institute Grants HL-17731 and HL-00111. I. Young was recipient of the Bushell Travelling Fellowship of the Royal Australasian College of Physicians and was also supported by the T. and E. M. Ewing Fellowship and Postgraduate Medical Foundation grants from the University of Sydney and the North Foundation.

Received 27 August 1979; accepted in final form 26 February 1980.

REFERENCES

1. BOUHUYS, A. Distribution of inspired gas in the lungs. In: *Handbook of Physiology. Respiration.* Washington, DC: Am. Physiol. Soc., 1964, sect. 3, vol. I, chapt. 28, p. 699–714.

2. CUMMING, G., K. HORSFIELD, J. G. JONES, AND D. C. F. MUIR. Inhomogeneity of ventilation in normal and abnormal lungs. In: *Form and Function in the Human Lung*, edited by G. Cumming

and L. B. Hunt. Edinburgh: Livingstone, 1968, p. 55–56.
3. DANTZKER, D. R., P. D. WAGNER, V. W. TORNABENE, N. P. ALAZRAKI, AND J. B. WEST. Gas exchange after pulmonary thromboembolization in dogs. *Circ. Res.* 42: 92–103, 1978.
4. DUECK, R., P. D. WAGNER, AND J. B. WEST. Effects of positive end-expiratory pressure on gas exchange in dogs with normal and edematous lungs. *Anesthesiology* 47: 359–366, 1977.
5. EVANS, J. W., AND P. D. WAGNER. Limits of $\dot{V}A/\dot{Q}$ distributions from analysis of experimental inert gas elimination. *J. Appl. Physiol.: Respirat. Environ. Exercise Physiol.* 42: 889–898, 1977.
6. HISLOP, A., AND L. M. REID. Formation of the pulmonary vasculature. In: *Development of the Lung*, edited by W. A. Hodson. New York: Dekker, 1977, p. 37–86.
7. HORSFIELD, K. Morphometry of the small pulmonary arteries in man. *Circ. Res.* 42: 593–597, 1978.
8. KEALEY, G. P., AND M. J. BRODY. Studies on the mechanism of pulmonary vascular responses to miliary pulmonary embolism. *Circ. Res.* 41: 807–814, 1977.
9. LEVY, S. E., AND D. H. SIMMONS. Mechanism of arterial hypoxemia following pulmonary thromboembolism in dogs. *J. Appl. Physiol.* 39: 41–46, 1975.
10. LEVY, S. E., AND D. H. SIMMONS. Redistribution of alveolar ventilation following pulmonary thromboembolism in the dog. *J. Appl. Physiol.* 36: 60–68, 1974.
11. MALIK, A. B., AND H. VAN DER ZEE. Time course of pulmonary vascular response to microembolization. *J. Appl. Physiol.: Respirat. Environ. Exercise Physiol.* 43: 51–58, 1977.
12. MALIK, A. B., AND H. VAN DER ZEE. Mechanism of pulmonary edema induced by microembolization in dogs. *Circ. Res.* 42: 73–79, 1978.
13. NIDEN, A. H., AND D. M. AVIADO, JR. Effects of pulmonary embolism on the pulmonary circulation with special reference to arteriovenous shunts in the lung. *Circ. Res.* 4: 67–73, 1956.
14. RHODIN, J. A. G. Microscopic anatomy of the vascular bed in the cat lung. *Microvasc. Res.* 15: 169–193, 1978.
15. WAGNER, P. D., R. B. LARAVUSO, E. GOLDZIMMER, P. F. NAUMANN, AND J. B. WEST. Distributions of ventilation-perfusion ratios in dogs with normal and abnormal lungs. *J. Appl. Physiol.* 38: 1099–1109, 1975.
16. WAGNER, P. D., R. B. LARAVUSO, R. R. UHL, AND J. B. WEST. Continuous distributions of ventilation-perfusion ratios in normal subjects breathing air and 100 percent O_2. *J. Clin. Invest.* 54: 54–68, 1974.
17. WAGNER, P. D., P. F. NAUMANN, AND R. B. LARAVUSO. Simultaneous measurement of eight foreign gases in blood by gas chromatography. *J. Appl. Physiol.* 36: 600–605, 1974.
18. WAGNER, P. D., H. A. SALTZMAN, AND J. B. WEST. Measurement of continuous distributions of ventilation-perfusion ratios: theory. *J. Appl. Physiol.* 36: 588–599, 1974.
19. WEST, J. B. *Ventilation/Blood Flow and Gas Exchange.* (2nd ed.). Oxford: Blackwell, 1972, p. 24.